Nine Years in the X-Ray Life of NGC 4258

Antonella Fruscione (CfA), Lincoln J. Greenhill (CfA), Alexei V. Filippenko (UCB), James M. Moran (CfA), James R. Herrnstein (Rentec), Elizabeth Galle (CfA)

2005, Astrophysical Journal, vol. 624, p. 103

We have analyzed X-ray (0.3-10 keV) observations of NGC 4258 obtained with the *XMM-Newton* and *Chandra* observatories. Including earlier observations by *ASCA* and *Beppo-SAX*, we present a new nine year time series of models fitted to the X-ray spectrum of NGC4258.

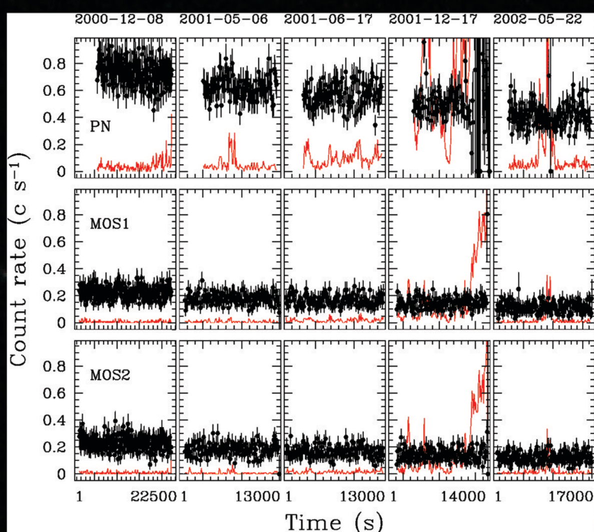

XMM EPIC background-subtracted light curves

- binned in 100 s bins for all five observation epochs. The red continuous lines represent the level of the background.
- The light curves were extracted for the nuclear region (15″ extraction radius) over the entire instrumental energy range (0.2-15 keV).
- During epoch 4 (2001-12-17) the observation was affected by strong background flares and a generally very high background level.
- Time spacing is *not* uniform between the different epochs.

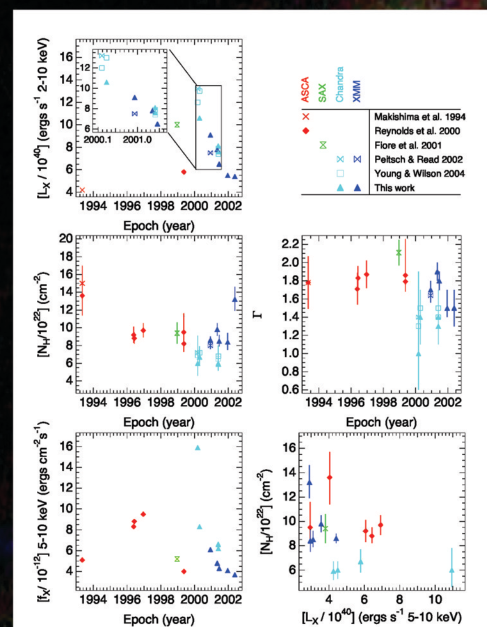

Time series of unabsorbed luminosity L_X, model column density (N_H), photon index (Γ), and absorbed flux (f_X)
(see table for definitions)

- Lower right panel: NH vs. hard Lx, which tracks the hard fX closely. No correlation is apparent, indicating that variations in flux are intrinsic to the central engine.
- Each dataset has been processed by more than one team. Plots of L_X (2-10 keV) and f_X (5-10 keV) are more sparse than plots of N_H and Γ because no single band is used throughout the literature.

MAIN CONCLUSIONS

1. XMM and Chandra spectra are well fit by a multi-components model: a partially absorbed, hard (2 keV) power law, a soft thermal plasma, and a soft power law. The soft emission, some of which arises <70 pc from the central engine, does not vary appreciably from observation to observation.
2. XMM data indicate long-term time variability in the source count rate and absorbed flux over time scales of 6 months. No evidence of variability on individual ~3 hour integrations.
3. From XMM data we detect a ~60% increase in N_H over ~5 months, returning to a high level not reported since the ASCA observations in 1993, N_H~1.3 x 10^{23} cm^{-2}.
4. Changes in N_H and f_X are not correlated, which indicates intrinsic variability of the central engine that is in one case 30% over 19 days (5-10 keV). We note that two of the largest estimates of unabsorbed luminosity are associated with the lowest estimates of N_H, and we speculate that reductions in L_X might affect the ionization state of the absorber.
5. The geometry and orientation of the accretion disk in NGC 4258 is well known from interferometric mapping of maser emission that arises in the accretion disk. The warped disk, a known source of H_2O maser emission, is believed to cross the line of sight to the central engine. Assuming that the absorbing gas lies in the disk, we propose that the variations in N_H arise from inhomogeneities sweeping across the line of sight in the rotating disk at the radius at which the disk crosses the line of sight. We estimate that the inhomogeneities are ~10^{15} cm in size at the crossing radius of 0.29pc. *This is the first direct confirmation that obscuration in type 2 AGNs may, in some cases, arise in thin, warped accretion disk rather than geometrically thick tori.*
6. We do not detect Fe Kα line emission in any of the XMM or Chandra epochs, thus extending the "disappearance" of the line from the last ASCA detection in May 1999 May to May 2002. The inferred line emission region is comparable in size to the maser disk. If the line arises from the disk (e.g., by fluorescence), then it is difficult to understand the variability because the maser emission has not changed substantially.
7. We do not observe evidence for absorption lines in any XMM or Chandra spectra.

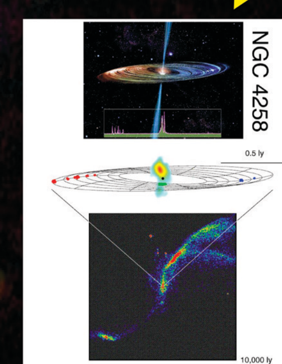

References

Fiore, F., et al. 2001, ApJ, 556, 150
Makishima, K., et al. 1994, PASJ, 45, L77
Miyoshi, M., et al. 1995, Nature, 373, 127
Pietsch, W., & Read, M. 2002, A&A, 384, 793
Reynolds, C. S., et al. 2000, ApJ, 540, 143
Young, A. J., & Wilson, A. S. 2004, ApJ, 601, 133

X-RAY SPECTRAL DATA FOR NGC4258

Observatory	Date	kT (keV)	$f_{0.5-2}$ (10^{-12})[a]	$L_{0.5-2}$ (10^{38})[b]	N_H (10^{22} cm^{-2})[c]	Γ_{pl}	f_{5-10} (10^{-12})[a]	L_{5-10} (10^{40})[b]	f_{2-10} (10^{-12})[a]	L_{2-10} (10^{40})[b]	E_{lin} (keV)	EW_{lin} (eV)	f_{lin} (10^{-13})[a]	Reference
ASCA	1993 May 5	0.5 ± 0.2[d,e]	...	...	15 ± 2	1.78 ± 0.29	...	...	...	4.2	6.5 ± 0.2	250 ± 100	...	1
	1993 May 5	...	...	...	$13.6^{+2.1}_{-2.2}$	$1.78^{+0.22}_{-0.26}$	5.1	4	...	...	...	...	...	2
ASCA	1996 May 23	...	...	...	9.2 ± 0.9	$1.71^{+0.18}_{-0.17}$	8.3	6.1	...	...	...	...	...	2
ASCA	1996 Jun 5	...	...	...	$8.8^{+0.7}_{-0.6}$	1.83 ± 0.13	8.8	6.4	...	...	...	...	...	2
ASCA	1996 Dec 18	...	...	...	9.7 ± 0.8	1.87 ± 0.15	9.5	6.9	...	...	...	...	...	2
BeppoSAX	1998 Dec 19	0.6 ± 0.1	1.6[d]	...	9.4 ± 1.2	2.11 ± 0.14	5.2	3.8	8	10	6.57 ± 0.20	85 ± 65	...	3
ASCA	1999 May 15	$0.47^{+0.03}_{-0.09}$	...	...	8.2 ± 0.9	$1.79^{+0.31}_{-0.11}$	...	...	...	5.8	...	...	...	2[f]
	1999 May 15	$0.36^{+0.03}_{-0.02}$	...	...	$9.5^{+2.1}_{-0.9}$	$1.86^{+0.40}_{-0.13}$	4.0	2.9	...	...	$6.45^{+0.10}_{-0.07}$	107^{+42}_{-37}	...	2[g]
Chandra	2000 Mar 8	...	...	...	7.2 ± 1.8	1.4 ± 0.5	...	...	14.4	13.2	...	...	...	4
	2000 Mar 8	N/A	N/A	N/A	$6.9^{+2.2}_{-1.8}$	1.3 ± 0.6	...	...	...	12	6.4	<887	...	5
	2000 Mar 8	N/A	N/A	N/A	$6.0^{+1.8}_{-1.4}$	$1.0^{+0.5}_{-0.4}$	15.9	11.0	21.2	17.4	6.4	<369	<12	6
Chandra	2000 Apr 17	$1.3^{+\infty}_{-0.9}$[e]	...	1.6	$7.2^{+0.7}_{-0.4}$	$1.5^{+0.1}_{-0.0}$	...	...	...	13	...	...	...	5
	2000 Apr 17[h]	0.5 ± 0.1	0.07	1.7	$6.7^{+1.0}_{-0.9}$	1.4 ± 0.3	8.3	5.8	11.8	10.6	6.4	<61	<1.2	6
XMM-Newton	2000 Dec 8	...	...	...	8.0 ± 0.4	1.64 ± 0.08	...	...	7.6	7.5	6.45	<40	...	4
	2000 Dec 8	0.6 ± 0.03	0.2	14.6	8.6 ± 0.4	1.7 ± 0.1	6.1	4.4	9.0	9.1	6.4	<69	<1.0	6
XMM-Newton	2001 May 6	$0.5^{+0.06}_{-0.05}$	0.2	15.3	9.8 ± 0.7	1.9 ± 0.1	4.8	3.5	7.1	7.8	6.4	<49	<0.6	6
Chandra	2001 May 28	$1.3^{+\infty}_{-0.8}$[e]	...	1.4	$6.5^{+0.6}_{-0.3}$	1.5 ± 0.1	...	...	...	7.9	6.4	<132	...	5
	2001 May 28[h]	$0.6^{+\infty}_{-0.18}$	0.06	1.3	6.0 ± 0.7	$1.4^{+0.3}_{-0.2}$	6.6	4.5	9.4	8.1	6.4	<191	<2.8	6
Chandra	2001 May 29	$1.0^{+0.6}_{-0.7}$[e]	...	1.5	$6.8^{+1.2}_{-1.0}$	1.4 ± 0.3	...	...	...	7.4	6.4	<94	...	5
	2001 May 29	0.8 ± 0.2	0.06	1.5	$5.9^{+0.8}_{-0.7}$	1.3 ± 0.2	6.2	4.3	8.8	7.6	6.4	<100	<1.4	6
XMM-Newton	2001 Jun 17	0.5 ± 0.05	0.2	14.1	$8.5^{+0.7}_{-0.6}$	1.8 ± 0.1	4.3	3.1	6.4	6.5	$6.3^{+0.07}_{-0.08}$[i]	66 ± 43[i]	0.7	6
XMM-Newton	2001 Dec 17	$0.5^{+0.06}_{-0.12}$	0.3	16.4	$8.4^{+1.0}_{-0.9}$	$1.5^{+0.2}_{-0.1}$	4.1	2.9	5.8	5.5	6.4	<67	<0.7	6
XMM-Newton	2002 May 22	0.5 ± 0.04	0.2	14.9	$13.2^{+1.4}_{-1.3}$	1.5 ± 0.2	3.7	2.8	4.9	5.4	6.4	<100	<0.9	6

NOTES.—Results reported here are from model fits performed on the 0.3–10 keV (*XMM-Newton*) and 0.5–10 keV (*Chandra*) energy ranges. The models comprise several components. For *Chandra* these are the Galactic absorption [N_H(gal) = 1.19×10^{20} cm^{-2}, frozen in the fits], intrinsic absorption (N_H), low-energy thermal plasma (kT), power-law (Γ_{pl}), and Gaussian Fe K line (E_{lin}, W_{lin}) components. For *XMM-Newton* an additional soft power law absorbed by N_H(gal) has also been added. The slope of this component remains almost constant in all observations with an average $\langle\Gamma\rangle = 1.6 \pm 0.2$. The energy of the Fe K line was frozen at 6.4 keV for all observations except that of *XMM-Newton* 2001 June 17. All errors are quoted at 90% confidence.

[a] Absorbed fluxes (ergs cm^2 s^{-1}) in the 0.5–2, 5–10, and 2–10 keV bands and Fe K line flux or upper limit. For *BeppoSAX* data, f_{5-10} is derived via Portable Interactive Multi-Mission Simulator (PIMMS) software, assuming the published values of f_{2-10}, N_H, and Γ_{pl}.

[b] Absorption-corrected luminosities (ergs s^{-1}) in the 0.5–2, 5–10, and 2–10 keV bands, assuming a distance of 7.2 Mpc. Both Galactic and intrinsic absorption have been removed. For *ASCA* and *BeppoSAX* data L_{5-10} is derived via PIMMS, assuming the values of f_{5-10}, N_H, and Γ_{pl}.

[c] Intrinsic equivalent hydrogen column density.

[d] The 0.1–2.4 keV energy band.

[e] Bremsstrahlung temperature.

[f] Model F (best fit) in Table 1 of Reynolds et al. (2000).

[g] Model G (with added Gaussian) in Table 1 of Reynolds et al. (2000). Note that there are some typographical errors in paragraph 3.2 of Reynolds et al. (2000): model D, model E, and model F should read model E, model F, and model G, respectively.

[h] A pileup model with α and *f* free to vary was added to the model components. See text and Table 3 for details.

[i] Values were obtained by leaving E_{lin} free to vary. The fit is not significantly improved by the addition of a Gaussian line (reduced $\chi^2 = 1.05$ for 159 dof without a line or reduced $\chi^2 = 1.02$ for 156 dof with a line).

REFERENCES.—(1) Makishima et al. 1994; (2) Reynolds et al. 2000; (3) Fiore et al. 2001; (4) Pietsch & Read 2002; (5) Young & Wilson 2004; (6) this work.

- **XMM EPIC spectra** of the nucleus (15″ extraction radius) of NGC4258.
- Data are "grouped" by 10 PI channels.
- PN, MOS1, and MOS2 data are fitted simultaneously with a model consisting of 2 power laws (dotted and dot-dashed lines) plus a thermal spectrum (dashed line) absorbed by intrinsic and Galactic gas (N_H).
- The best fit is the red solid line.
- Residuals (in units of σ) are shown for all instruments.

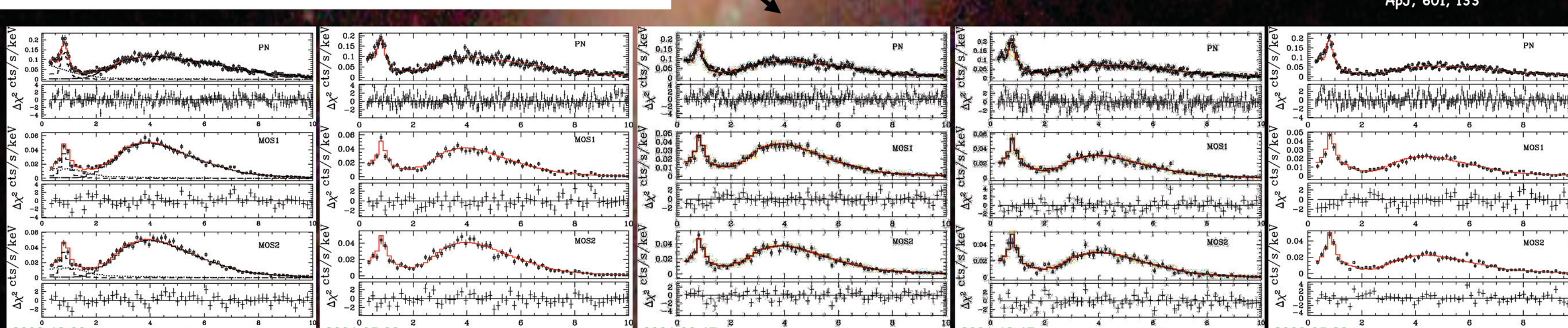

- **Chandra ACIS spectra** of the nucleus (2″ extraction radius) of NGC 4258.
- Data "grouped" by 10 PI channels.
- Data fitted with a model consisting of a power law plus a thermal component absorbed by intrinsic and Galactic gas N_H.
- Pileup included in modeling.